

Validation of *Plasmodium falciparum* deoxyhypusine synthase as an antimalarial target

Aiyada Aroonsri¹, Navaporn Posayapisit¹, Jindaporn Kongsee²,
Onsiri Siripan^{1,3}, Danoo Vitsupakorn¹, Sugunya Utaida²,
Chairat Uthaipibull¹, Sumalee Kamchonwongpaisan¹ and
Philip J. Shaw¹

¹ Protein-Ligand Engineering and Molecular Biology Laboratory, Medical Molecular Biology Research Unit, National Center for Genetic Engineering and Biotechnology (BIOTEC), National Science and Technology Development Agency (NSTDA), Pathum Thani, Thailand

² Department of Biotechnology, Faculty of Science and Technology, Thammasat University, Pathum Thani, Thailand

³ Present address: Fisheries Industrial Technology Research and Development Division, Department of Fisheries, Bangkok, Thailand

ABSTRACT

Background: Hypusination is an essential post-translational modification in eukaryotes. The two enzymes required for this modification, namely deoxyhypusine synthase (DHS) and deoxyhypusine hydrolase are also conserved. *Plasmodium falciparum* human malaria parasites possess genes for both hypusination enzymes, which are hypothesized to be targets of antimalarial drugs.

Methods: Transgenic *P. falciparum* parasites with modification of the PF3D7_1412600 gene encoding *PfDHS* enzyme were created by insertion of the *glmS* riboswitch or the M9 inactive variant. The *PfDHS* protein was studied in transgenic parasites by confocal microscopy and Western immunoblotting. The biochemical function of *PfDHS* enzyme in parasites was assessed by hypusination and nascent protein synthesis assays. Gene essentiality was assessed by competitive growth assays and chemogenomic profiling.

Results: Clonal transgenic parasites with integration of *glmS* riboswitch downstream of the *PfDHS* gene were established. *PfDHS* protein was present in the cytoplasm of transgenic parasites in asexual stages. The *PfDHS* protein could be attenuated fivefold in transgenic parasites with an active riboswitch, whereas *PfDHS* protein expression was unaffected in control transgenic parasites with insertion of the riboswitch-inactive sequence. Attenuation of *PfDHS* expression for 72 h led to a significant reduction of hypusinated protein; however, global protein synthesis was unaffected. Parasites with attenuated *PfDHS* expression showed a significant growth defect, although their decline was not as rapid as parasites with attenuated dihydrofolate reductase-thymidylate synthase (*PfDHFR-TS*) expression. *PfDHS*-attenuated parasites showed increased sensitivity to *N*¹-guanyl-1,7-diaminoheptane, a structural analog of spermidine, and a known inhibitor of DHS enzymes.

Discussion: Loss of *PfDHS* function leads to reduced hypusination, which may be important for synthesis of some essential proteins. The growth defect in parasites with attenuated *PfDHS* expression suggests that this gene is essential. However,

Submitted 9 August 2018

Accepted 5 March 2019

Published 17 April 2019

Corresponding author

Philip J. Shaw, philip@biotec.or.th

Academic editor

Erika Braga

Additional Information and
Declarations can be found on
page 20

DOI 10.7717/peerj.6713

© Copyright

2019 Aroonsri et al.

Distributed under

Creative Commons CC-BY 4.0

OPEN ACCESS

the slower decline of *PfDHS* mutants compared with *PfDHFR-TS* mutants in competitive growth assays suggests that *PfDHS* is less vulnerable as an antimalarial target. Nevertheless, the data validate *PfDHS* as an antimalarial target which can be inhibited by spermidine-like compounds.

Subjects Biochemistry, Cell Biology, Microbiology, Molecular Biology, Parasitology

Keywords Hypusination, *glmS* riboswitch, *PfDHS*, Deoxyhypusine synthase, *Plasmodium falciparum*, *PfeIF5A*, Antimalarial, Drug target

INTRODUCTION

The incidence of malaria has declined around the world in recent years, with a 21% reduction reported worldwide during the period 2010–2015 (*World Health Organization, 2016*). Programs to eliminate the disease in endemic countries could be thwarted by evolving *Plasmodium falciparum* parasite resistance to artemisinin-combination therapies that are widely used to treat and prevent infections (*Woodrow & White, 2017*). New drugs with novel modes of action are needed to combat drug-resistant parasites. Identification of novel drug targets should accelerate the development of such antimalarials.

Polyamines are nitrogenous base compounds that are essential for cellular proliferation and development. Malaria parasites synthesize large amounts of polyamines, in which spermidine is a major metabolite present in all stages of development (*Teng et al., 2009*). Moreover, several different polyamine analogues possess antimalarial activity, suggesting that polyamine metabolism constitutes novel drug targets (reviewed in *Clark et al. (2010)*). One of the main uses of spermidine in eukaryotes is for hypusination of translation initiation factor 5A (eIF5A) protein; two enzymes are required for this post-translational modification, namely deoxyhypusine synthase (DHS) and deoxyhypusine hydrolase (reviewed in *Park et al. (2010)*). *P. falciparum* possesses a single gene encoding eIF5A, and functional studies of the parasite eIF5A protein have shown that it is a substrate for hypusination (*Molitor et al., 2004*). Malaria parasites also possess canonical enzymes for hypusination of eIF5A, and the *P. falciparum* DHS enzyme (*PfDHS*) uses eIF5A protein as a substrate for incorporation of spermidine (*Kaiser et al., 2007*). The enzymatic activity of *PfDHS* is inhibited by *N*¹-guanyl-1,7-diaminoheptane (GC7), a known inhibitor of human DHS enzyme (*Kaiser et al., 2007*). Hypusination of eIF5A by *PfDHS* is likely to be essential since *P. falciparum* is moderately sensitive to growth inhibition by GC7 (*Kaiser et al., 2001*) and no insertions of *piggyBac* transposon within the *PfDHS* gene are tolerated (*Zhang et al., 2018*). The orthologous gene encoding DHS enzyme in the murine malaria parasite *P. berghei* is essential, since clonal transgenic *P. berghei* parasites with knockout of the DHS gene cannot be isolated (*Kersting et al., 2016*), and *P. berghei* DHS knockout parasites have a severe growth defect causing them to rapidly disappear from host animals co-infected with other transgenic parasites (*Bushell et al., 2017*).

In this study, we investigated *PfDHS* function in transgenic *P. falciparum* parasites. The *glmS* riboswitch tool (*Prommana et al., 2013*) was used to attenuate *PfDHS*

expression. Attenuation of *PfDHS* expression led to defects in hypusination of eIF5A and growth of transgenic parasites. Moreover, attenuation of *PfDHS* expression specifically sensitized parasites to GC7, a known inhibitor of *PfDHS* enzyme activity.

MATERIALS AND METHODS

Ethics statement

Human erythrocytes were obtained from donors after providing informed written consent, following a protocol approved by the Ethics Committee, National Science and Technology Development Agency, Pathum Thani, Thailand, document no. 0021/2560.

Construction of DNA transfection vectors

A total of 1,493 bp of homologous targeting sequence from the PF3D7_1412600 gene encoding deoxyhypusine synthase (*PfDHS*) was PCR-amplified from *P. falciparum* strain 3D7 genomic DNA using primers pGFP_glmS_DHSF and GFP_glmS_DHSR (Table S1) and Phusion[®] DNA polymerase (Thermo Fisher Scientific, Waltham, MA, USA) following the manufacturer's recommendations. The pGFP_glmS and pGFP_M9 plasmids carrying *glmS* riboswitch element and the M9 inactive variant, respectively, (Prommana *et al.*, 2013) were first modified to remove unnecessary hsp86 promoter and REP20 sequences by digestion with AflIII and BglII. The digested plasmids were religated to create Sim_pGFP_glmS and Sim_pGFP_M9 vectors. The *PfDHS* targeting sequence was cloned into NheI and KpnI (New England Biolabs [NEB], Ipswich, MA, USA) digested vectors using a Gibson assembly kit (NEB). A total of 960 bp of homologous targeting sequence from the PF3D7_1364900 gene encoding ferrochelatase (*PfFC*) was PCR-amplified from *P. falciparum* strain 3D7 genomic DNA using primers PffCSacIIF and PffCKpnIR (Table S1) and GoTaq[®] DNA polymerase (Promega Corporation, Madison, WI, USA) following the manufacturer's recommendations. The *PfFC* targeting sequence DNA was digested with SacII and KpnI restriction enzymes (NEB) and cloned into pGFP_glmS plasmid (Prommana *et al.*, 2013) digested with the same enzymes.

Plasmodium falciparum culture and DNA transfection

Plasmodium falciparum strain 3D7 (reference strain) and transgenic parasite derivatives were cultured in vitro following the standard method (Trager & Jensen, 1976), with the modification of 0.5% Albumax I (Gibco[™], Thermo Fisher Scientific, Waltham, MA, USA) replacing human serum (Cranmer *et al.*, 1997). Human O+ erythrocytes were obtained from donors after obtaining their written informed consent. 2% hematocrit was used for most parasite cultures, with slightly higher hematocrit (up to 4%) used during blasticidin selection steps of DNA transfection. Parasites were synchronized to ring stages by sorbitol treatment (Lambros & Vanderberg, 1979). Approximately 50 µg of plasmid DNA was used for each parasite transfection experiment. Transfection was performed by the method of direct transfection of infected host cells (Wu *et al.*, 1995) or invasion of DNA-loaded erythrocytes (Deutsch, Driskill & Wellem, 2001). Transgenic parasites were selected by treatment with 2 µg/mL blasticidinS-HCl (Gibco[™]), which was added to parasite culture 48 h post-transfection. Parasites were cultured under drug

selection until resistant parasites emerged (3 weeks), after which the drug was removed and culture continued for 2 weeks. The drug on-off cycle (2 weeks each) was repeated to enrich for integrant parasites in the population. Integrants were detected by PCR assay. Genomic DNA samples were obtained for genotypic analysis of transgenic parasites using a Genomic DNA Mini Kit (Blood/Cultured Cell) (Geneaid Biotech, New Taipei City, Taiwan). Integration at the *PfDHS* locus was checked using primers DHS_intF and 3UTRpBDT_glmSR (Table S1). PCRs contained 20 ng of genomic DNA, 500 nM of each primer, one unit of Phusion polymerase (Thermo Scientific™, Thermo Fisher Scientific, Waltham, MA, USA) and 2.5 mM MgCl₂. The reaction conditions were: 98 °C for 3 min followed by 35 cycles of 98 °C 10 s, 52 °C 30 s, and 72 °C for 90 s, and final extension at 72 °C for 5 min. The presence of transfected DNA in transfection experiments to modify the *PfFC* gene was checked using primers BglIIPfFCF and 3UTRpBDTglmSR (Table S1). A control PCR to amplify the *PfFC* coding region and thus verify template DNA quality was performed using primers BglIIPfFCF and PffCKpnIR (Table S1). PCR assays of the *PfFC* locus contained 20 ng of genomic DNA, 100 nM of each primer, one unit of GoTaq polymerase (Promega Corporation), and 2.5 mM MgCl₂. The reaction conditions were: 95 °C for 2 min followed by 30 cycles of 95 °C 45 s, 53 °C 45 s, and 62 °C for 2 min 30 s, and final extension at 62 °C for 5 min.

Clonal lines of integrant transgenic parasites were established by limiting dilution in 96-well culture plates. A single clonal line from each transfection experiment, verified as integrant, was randomly selected for further study. Clonal lines *PfDHS_glmS* (active riboswitch) and *PfDHS_M9* (inactive riboswitch) with integration at the *PfDHS* locus were obtained (Fig. S1). The clonal line *PfFC_glmS* (active riboswitch) with integration at the *PfFC* locus was obtained. Plasmid integration in clonal transgenic lines was verified by Southern blot (Figs. S1 and S2). A total of 20 µg samples of genomic DNA were digested overnight with restriction enzymes (NEB). BamHI and AflII enzymes were used for the *PfDHS* locus and SpeI and HindIII enzymes were used for the *PfFC* locus. Digested DNA samples were separated by electrophoresis and transferred by capillary action to Hybond N+ nylon membrane (GE Healthcare, Chicago, IL, USA). Probes were synthesized by PCR using primers pGFP_glmS_DHSF and GFP_glmS_DHSR for the *PfDHS* locus, and PffCSacIIF and PffCKpnIR for the *PfFC* locus (Table S1) as described above. Probe labeling, hybridization, and detection were performed using a DIG High Prime DNA labeling and Detection Starter Kit II (Roche Diagnostics, Basel, Switzerland) following the manufacturer's instructions. The integrant transgenic parasite line described in (Prommana et al., 2013), referred to here as *PfDHFR-TS_glmS*, was used for growth studies. This parasite has a modified PF3D7_0417200 gene encoding *P. falciparum* dihydrofolate reductase-thymidylate synthase (*PfDHFR-TS*) with integration of GFP and *glmS* riboswitch sequences.

Confocal microscopy

Specimens of transgenic parasites *PfDHS_glmS*, *PfFC_glmS*, *PfDHFR-TS_glmS*, and 3D7 parental parasites were analyzed on a model FV 1,000D IX81 confocal laser scanning microscope (Olympus, Shinjuku, Japan). A 100× oil immersion objective lens (1.4 NA)

was used. Parasite mitochondria were stained with 1 mM Mitotracker (Invitrogen™, Carlsbad, CA, USA; Thermo Fisher Scientific, Waltham, MA, USA) for 45–60 min at 37 °C. Parasite nuclei were stained with Hoechst 33342 (Invitrogen™) diluted 1:1,000 in RPMI medium (Gibco™) for 5 min at 37 °C. GFP signal was detected with an Argon laser 488 nm (500 nm excitation/600 nm emission; laser power 15%; high detector sensitivity 741 V; gain = 1 and offset = 12%), Mitotracker signal was detected with a yellow diode laser 559 nm (575 nm excitation/675 nm emission; laser power 15%; high detector sensitivity 641 V; gain = 1 and offset = 0%), and Hoechst signal was detected with a UV laser diode 405 nm (425 nm excitation/475 nm emission; laser power 10%; high detector sensitivity 615 V; gain = 1, and offset = 14%). Images were obtained using a scan speed of 10.0 μs/pixel and were analyzed using FV10-ASW 3.0 Viewer software (Olympus, Shinjuku, Japan).

Western immunoblot of *PfDHS-GFP* protein

A total of 15 mL cultures of ring-stage *PfDHS_glmS* and *PfDHS_M9* synchronized parasites at 5% parasitemia and 3% haematocrit were treated with 0, 1.25, 2.5, and 5.0 mM GlcN for 24 h and harvested. Parasites were liberated from host cells by saponin lysis and washed with 1× PBS buffer (Thermo Scientific™) containing 1× EDTA-free protease inhibitor cocktail (Sigma-Aldrich, Merck KGaA, Germany) and 0.7 μg/mL pepstatin (Sigma). Parasite proteins were extracted by freeze-thaw rupture. Protein lysate was diluted in NuPAGE™ LDS sample buffer (4×, Thermo Scientific™) and stored at –80 °C. A 10 μg sample from each protein lysate was separated in NuPAGE 4–12% Bis-Tris Protein Gel (Invitrogen™) with 1× NuPAGE MOPS SDS running buffer (Invitrogen™). Proteins were transferred for 1.5 h at 30 V onto Immobilon-P PVDF membrane (Merck-Millipore, Merck KGaA, Germany) in 1× NuPAGE transfer buffer (Invitrogen™) by using a XCell II Blot system (Invitrogen™). Total protein was detected by Ponceau-S (Sigma) staining and an image of the stained membrane was captured on a flatbed scanner. After scanning, the Ponceau-S stain was removed from the membrane by washing with water. The destained membrane was incubated in blocking solution (5% non-fat skimmed milk in 1× TBST buffer; 10 mM Tris-base, 15 mM NaCl, pH 8.0, 0.05% Tween 20) for 1 h. *PfDHS-GFP* protein was immunodetected with 1:5,000 dilutions of rabbit anti-GFP polyclonal antibody (#PA1-19431; Thermo Scientific™) and goat anti-rabbit IgG antibody conjugated with HRP (#SC-2004; Santa-Cruz Biotechnology, Dallas, TX, USA). Proteins were detected by chemiluminescence using Pierce ECL Western Blotting Substrate (Thermo Scientific™). The intensity of the *PfDHS-GFP* band was measured by densitometry from the scanned image of the exposed X-ray film using the Image J program (Schneider, Rasband & Eliceiri, 2012). The immunodetected protein band signals were normalized to total protein signal in each lane. The percent relative intensities of *PfDHS-GFP* are intensities in GlcN treatment conditions relative to the untreated control.

Western immunoblot of *PfDHFRTS-GFP* and *PfFC-GFP* protein

PfFC_glmS, *PfDHFRTS_glmS*, and 3D7 parasites were cultured and synchronized as described above and harvested at the trophozoite stage. Parasites were liberated from erythrocytes by saponin lysis. Parasites were resuspended in 1× NuPAGE LDS sample

buffer in a ratio of parasite cell/buffer volume of 2×10^6 parasites/mL and incubated at 95°C for 10–15 min for protein extraction. Insoluble material was separated by centrifugation. Protein samples from 1×10^6 , 5×10^6 , 10×10^6 , or 25×10^6 parasites were separated by electrophoresis as described above for *PfDHS-GFP* Western immunoblot. Precision Plus Protein™ Dual Color Standards (Bio-Rad, Hercules, CA, USA) were used as a protein ladder. Proteins were transferred to Immobilon-FL PVDF membrane (Merck) as described above for *PfDHS-GFP* Western immunoblot. After transfer, membranes were stained with REVERT™ Total Protein Stain (LI-COR Biosciences, Lincoln, NE, USA). Total protein was visualized using an Odyssey® CLx system (LI-COR) in the 700 nm channel. After imaging, REVERT stain was removed by washing with REVERT Reversal Solution (LI-COR) and water. The membrane was then incubated in Odyssey blocking buffer (TBS) (LI-COR) for 1 h with 80 rpm shaking. The blocked membrane was incubated in Odyssey blocking buffer (TBS) with 0.2% (v/v) Tween 20 and 1:2,000 diluted rabbit anti-GFP polyclonal antibody (#G1544; Sigma) overnight with 80 rpm shaking. The membrane was then washed with $1 \times$ TBST ($1 \times$ TBS with 0.05% Tween 20) and incubated in Odyssey blocking buffer (TBS) with 0.2% Tween 20 and IRDye 800CW 1:20,000 diluted goat anti-rabbit IgG (LI-COR) for 1 h at room temperature in the dark. The membrane was scanned in the 800 nm channel and images were analyzed using Image Studio Software (LI-COR).

Hypusination assay

A total of 10 mL *P. falciparum* sorbitol-synchronized cultures at approximately 2% hematocrit and 1% ring-stage parasitemia were treated with 0, 2.5, or 5.0 mM GlcN for 72 h. Parasites were harvested and liberated from erythrocytes by saponin lysis. Parasite pellets were resuspended in 1% Triton-X100 in $1 \times$ PBS buffer and incubated at 4°C for 20 min to extract protein. Protein samples from approximately 5×10^6 parasites were separated by electrophoresis as described above for *PfDHS-GFP* Western immunoblot. Precision Plus Protein Kaleidoscope Prestained Protein Standards (Biorad) were used as a protein ladder. Proteins were transferred to Immobilon-FL PVDF membrane (Merck) and processed before detection with Odyssey CLx as described above. The blocked membrane was incubated in Odyssey blocking buffer (TBS) with 0.2% (v/v) Tween 20 and 1:5,000 diluted rabbit anti-hypusine polyclonal antibody (#ABS1064; Merck) for 1 h with 80 rpm shaking. The membrane was then washed with $1 \times$ TBST ($1 \times$ TBS with 0.05% Tween 20) and incubated in Odyssey blocking buffer (TBS) with 0.2% Tween 20 and IRDye 680RD Goat anti-Rabbit IgG (LI-COR) for 1 h at room temperature in the dark. The membrane was scanned in the 700 nm channel and images were analyzed using Image Studio Software (LI-COR). Total protein loading in each lane was quantified by the sum of pixels minus background in rectangular objects spanning polypeptides 15–150 kDa. The major band of hypusinated protein signal assumed to be *PfeIF5A* (17.6 kDa) was normalized to the total protein signal in each lane and expressed relative to the control lane (zero mM GlcN treatment).

Nascent protein synthesis (puromycilation) assay

Nascent protein synthesis was assessed using the puromycilation assay ([Schmidt et al., 2009](#)). This assay is based on the incorporation of the translation inhibitor puromycin into

nascent peptide chains by actively translating ribosomes (Nathans, 1964). A previous report showed that this assay is suitable for *P. falciparum* (McLean & Jacobs-Lorena, 2017). Synchronized *P. falciparum* cultures were treated with GlcN for 72 h as described above for hypusination assay. After GlcN treatment, puromycin (Sigma) was added to a final concentration of 5 μ M and parasites were incubated at 37 °C for an additional 10 min. The parasitized red blood cells were then washed with incomplete medium and parasites were liberated from erythrocytes by saponin lysis. Protein samples were obtained from approximately 5×10^6 parasites, separated by electrophoresis, transferred to PVDF membrane and processed before detection as described above for hypusination assay. After blocking, the membrane was incubated in Odyssey blocking buffer (TBS) with 0.2% (v/v) Tween 20 and 1:10,000 diluted mouse anti-puromycin monoclonal antibody clone 12D10 (Merck) for 1 h with 80 rpm shaking. The membrane was washed with 1 \times TBST (1 \times TBS with 0.05% Tween 20) and incubated in Odyssey blocking buffer (TBS) with 0.2% Tween 20, IRDye 800CW Goat anti-Mouse IgG (LI-COR) for 1 h at room temperature in the dark. The membrane was washed with 1 \times TBST (1 \times TBS with 0.05% Tween 20) and 1 \times TBS buffer before scanning in the 800 nm channel. Total protein and puromycolated peptides in each lane were quantified by the sum of pixels minus background in rectangular objects spanning polypeptides 15–150 kDa. The puromycolated peptide signal was normalized to the total protein signal in each lane and expressed relative to the control lane (zero mM GlcN treatment). The puromycolation assay was validated using *P. falciparum* synchronized cultures at mostly trophozoite stage. Parasites were pre-treated with growth-inhibitory compounds cycloheximide (1, 10, or 100 μ M); dihydroartemisinin (0.01, 0.10, or 1 μ M), and GC7 (50, 100, or 1,000 μ M) for 1 h prior to puromycin exposure.

Competitive growth assay

P. falciparum transgenic parasite line *PfFC_glmS* was used as a control. The growth of a test transgenic line with riboswitch element integrated at a putative essential gene was normalized to that of the *PfFC_glmS* control. The control and test transgenic lines were first cultured separately and synchronized as described above. Ring-stage synchronized parasites were diluted to approximately 0.5% parasitemia. A new culture was established by combining control and test transgenic parasite cultures (5 mL of each) into the same culture plate. Samples were taken from the parasite co-culture every 4 days for 21 days (10 growth cycles). At each sampled time-point, the culture reached a parasitemia of approximately 2.5%, consisting of mostly trophozoite stage parasites. The culture was then diluted to approximately 0.1% parasitemia in fresh medium. The parasite culture plates were placed in a refrigerator on “ring” days for 5–7 h to maintain high synchronization (Yuan *et al.*, 2014). Parasite pellets were harvested and used for genomic DNA extraction. The co-culture was conducted under standard and gene attenuation (2.5 or 5.0 mM GlcN inducer added) conditions, in which fresh GlcN was added after each time-point. The effect of GlcN on development of control parasites 3D7 and *PfFC_glmS* was assessed by counting ring and trophozoite stage parasites separately from Giemsa-stained thin smears.

Quantitative PCR assay of transgenic parasite ratios in competitive growth experiments

Primers for quantitative PCR (qPCR) assays were designed to amplify specific discriminatory sequences in transgenic parasites tested in competitive growth assays. The discriminatory sequences spanned the fusion boundary between the 3' end of the modified target gene and the GFP coding region. The LDH-F and LDH-R primers (Table S1; amplicon 221 bp) were also designed to amplify the PF3D7_1324900 (L-lactate dehydrogenase) gene, which is present at single copy in all parasites and is used for normalization of template DNA input. qPCR experiments were performed using a CFX96 Touch Real-Time PCR Detection System (Biorad) and SsoFast EvaGreen Supermix (Biorad) in 20 μ L reaction volumes, as recommended by the manufacturer. All primer pairs performed with similar efficiency (96–103%, linear regression $R^2 > 0.99$). Amplicons of the expected size were obtained only from the expected template genomic DNA, as assessed by agarose gel electrophoresis and melt-curve analysis. The *PfDHS_glmS* and *PfDHS_M9* parasites were quantified from the DHS-GFP amplicon (188 bp, primers DHS-F and DHS-R; Table S1), the *PfDHR-TS_glmS* parasite (Prommana et al., 2013) was quantified from the TS-GFP amplicon (190 bp, primers DHFRTS-F and DHFRTS-R; Table S1), and the *PfFC_glmS* parasite was quantified by the FC-GFP amplicon (125 bp, primers FC-F and FC-R; Table S1). The quantitative range of qPCR assays was determined using purified genomic DNA extracted from transgenic parasites that were mixed in different ratios (Fig. S3).

Dose-response growth inhibition assays

The growth of parasites was monitored under different concentrations of growth inhibitors in dose-response assays as described previously (Aroonsri et al., 2016). To assess the effect of GlcN on growth inhibition, parasites were co-treated with 2.5 mM GlcN. The growth inhibitory compounds tested included *N*¹-guanyl-1,7-diaminoheptane (GC7; Sigma), cycloheximide (CYC; Sigma), and pyrimethamine (PYR; Sigma). Stock solutions of growth inhibitors were prepared fresh for each experiment, in which compounds were dissolved in DMSO (CYC and PYR) or culture medium (GC7). Compounds were diluted in culture medium, in which the maximum concentration of DMSO did not exceed 0.1%. Control wells with no growth inhibitory compound contained 0.1% DMSO.

Statistical analysis

All statistical analysis was performed using R 3.4.3 (R Core Team, 2017). For analysis of Western immunoblot, hypusination, and puromycylation assay data, Welch's two-tailed one-sample *t*-tests (Welch, 1947) were performed by testing the null hypothesis that sample means of test signal normalized to untreated control was not different from one. Tests with $P < 0.05$ were considered significant.

The lme4 package (Bates et al., 2015) was used to perform a linear mixed effects analysis of the relationship between parasite growth and time in competitive growth assays. For validation experiments with 3D7 parental and *PfFC_glmS* control transgenic lines, the percentage of ring or trophozoite-infected cells was taken as the growth variable.

In experiments with *PfDHFR-TS-glmS*, *PfDHS_glmS*, and *PfDHS_M9* transgenic parasites, growth relative to the *PfFC-glmS* control transgenic parasite determined by qPCR was taken as the growth variable. GlcN treatment (with doses as factors) was modeled as a fixed effect. Individual parasite cultures grown on different days were modeled as random effects, with random intercepts included in the model for the effect on growth over time. Linear models were constructed from the data using maximum likelihood. The null model was that growth varies as a function of time. The full model was that growth varies as a function of time, with GlcN treatment and its interaction with time as fixed effects. Significant differences in model fitting were assessed by likelihood ratio test, with $P < 0.05$ considered significant. Fitted models were plotted using the visreg package (Breheny & Burchett, 2017).

Normalized growth values from dose-response assays were analysed using the drc package (Ritz & Streibig, 2005). To allow proper comparison of EC_{50} values between the –GlcN and +GlcN conditions, the maximum and minimum growth values were assigned as shared and constant between the two conditions, such that only two parameters (slope and EC_{50}) varied between the –GlcN and +GlcN conditions. EC_{50} ratios, associated S.Es and t -statistics were calculated from the two-variable parameter fitted models using the EDcomp function in the drc package. EC_{50} ratios were considered significant at $P < 0.001$.

In silico modeling of *PfDHS* protein structure and GC7 binding

A three-dimensional structure of the *PfDHS* tetramer was constructed by the SWISS-MODEL Server (Waterhouse et al., 2018). The program selected the X-ray crystal structure of Form I human DHS complexed with NAD as the homology template (Umland et al., 2004); PDB ID: 1RLZ. Ligand binding site identification and characterization was performed using SiteMap version 3.6, Schrödinger, LLC, New York (Halgren, 2009). The grid type was set as coarse and other settings were default. The putative ball-and-chain motif encompassing residues Ile30–Pro45 of each *PfDHS* subunit was removed prior to ligand binding site analysis. Ligand binding sites with scores greater than 1.0 were considered significant. Molecular docking of GC7 at the substrate-binding pocket was performed using Glide (Friesner et al., 2004). A grid receptor was generated around the binding pocket with addition of void volume around NAD cofactor. The structure of Form II human DHS complexed with NAD and GC7 (Umland et al., 2004); PDB ID: 1RQD was used for comparison of *PfDHS* and human DHS substrate binding pockets.

RESULTS

Clonal transgenic *P. falciparum* parasite lines *PfDHS_glmS* and *PfDHS_M9* were established with integration of *glmS* riboswitch and the M9 inactive variant, respectively, at the *PfDHS* encoding gene PF3D7_1412600. The DNA vectors used for integration also contain GFP gene sequence for C-terminal tagging of the target protein. Fluorescent parasites with GFP signal in the parasite cytoplasm were observed in ring, trophozoite, and schizont stages for the *PfDHS_glmS* parasite (Fig. 1). Western immunoblotting with anti-GFP antibody revealed a species that migrated slightly larger than predicted for *PfDHS*-GFP fusion protein (85.1 kDa) from *PfDHS_glmS* and *PfDHS_M9* parasites

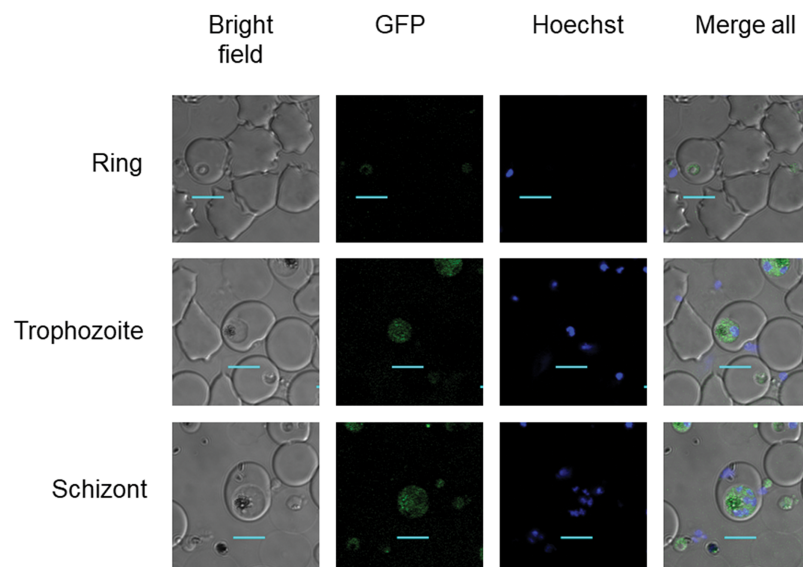


Figure 1 *PfDHS* protein localization in transgenic parasites. Representative confocal microscopic images of *PfDHS_glmS* parasites expressing GFP-tagged *PfDHS* protein at ring, trophozoite, and schizont stages. Parasite nuclei were stained with Hoechst 33342. Composite images from merging Hoechst and GFP fluorescence signals with the Bright-field image are shown in the panels on the far-right. Scale bars = 5 μ m. [Full-size !\[\]\(1663bb69f307a960345edb0e712f8c02_img.jpg\) DOI: 10.7717/peerj.6713/fig-1](https://doi.org/10.7717/peerj.6713/fig-1)

(Fig. 2). *PfDHS*-GFP protein was significantly attenuated in the *PfDHS_glmS* parasite treated for 24 h with GlcN, with up to fivefold reduction observed with 5.0 mM GlcN. In contrast, no significant reduction of *PfDHS*-GFP protein was observed with GlcN treatment in the *PfDHS_M9* parasite with an inactive riboswitch.

Since the primary function of DHS enzyme in eukaryotes is hypusination of eIF5A protein, hypusination was quantified using a commercial anti-hypusine antibody in transgenic parasites. A major protein species (<20 kDa) was detected by Western immunoblotting with this antibody which matches the predicted molecular weight of *P. falciparum* eIF5A (17.6 kDa) and is the approximately the same size as *PfeIF5A* detected with anti-eIF5A antibodies (Foth et al., 2008). However, additional evidence, for example, peptide mapping is needed to confirm that this species is *PfeIF5A*. GlcN treatment led to significantly reduced hypusinated protein signal in *PfDHS_glmS* parasites treated with GlcN compared with untreated controls, although this effect was rather small with <30% mean reduction at 5.0 mM GlcN (Fig. 3). In contrast, GlcN treatment had no significant effect on hypusination in *PfDHS_M9* parasites. We infer from this result that reduction of *PfDHS* expression leads to concomitant reduction of hypusinated protein. Hypusination is thought to be essential for the translation elongation function of this protein (Park et al., 2010). We tested whether reduced hypusination could affect protein synthesis by nascent protein synthesis (puromycylation) assay in *PfDHS_glmS* and *PfDHS_M9* parasites. Nascent protein was quantified by the incorporation of puromycin into elongating peptide chains, detected as the signal from Western immunoblotting with anti-puromycin antibody. Short pre-treatments of parasites with lethal (>EC₅₀) concentrations of CYC and DHA known to cause arrest of protein synthesis in

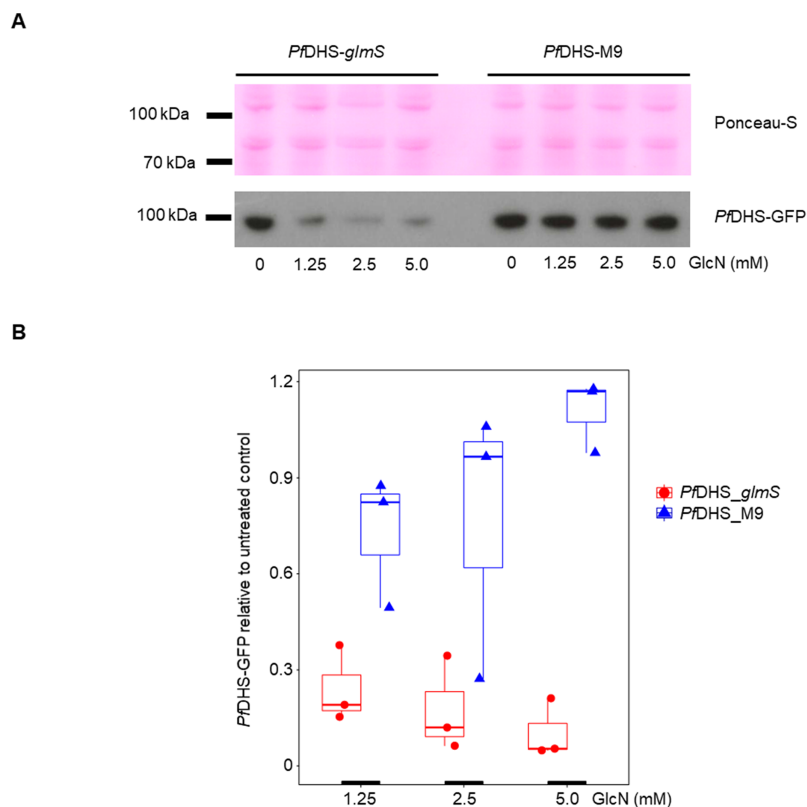


Figure 2 Attenuation of *PfDHS* expression in transgenic parasites. (A) Representative Western immunoblot results from detection of GFP-tagged *PfDHS* protein (*PfDHS-GFP*) in *PfDHS_glmS* and *PfDHS_M9* transgenic parasites. Soluble protein extracts were obtained from approximately 10×10^6 parasites treated for 24 h with 0, 1.25, 2.50, and 5.00 mM glucosamine (GlcN). Proteins were separated in 4–12% NuPAGE gel and transferred to PVDF membrane. Total protein was stained on the membrane using Ponceau-S (top panel) and *PfDHS-GFP* protein was detected using anti-GFP antibody (bottom panel). The migrations of PageRuler Plus Prestained Protein ladder (Thermo Scientific, Waltham, MA, USA) standards are indicated on the left. The images are cropped for clarity. Full-length, uncropped blot images are shown in Fig. S4. (B) Quantified Western immunoblot results. The signal intensity of the *PfDHS-GFP* protein band was normalized to the total protein and the *PfDHS-GFP* protein signal intensity in the sample lane from untreated parasites. The data from three independent experiments are shown for each parasite line. *P*-values from one-sample *t*-tests: 0.0082 (*PfDHS_glmS*, 1.25 mM GlcN); 0.011 (*PfDHS_glmS*, 2.5 mM GlcN); 0.0035 (*PfDHS_glmS*, 5.0 mM GlcN); 0.15 (*PfDHS_M9*, 1.25 mM GlcN); 0.45 (*PfDHS_M9*, 2.5 mM GlcN), and 0.24 (*PfDHS_M9*, 5.0 mM GlcN).

Full-size DOI: 10.7717/peerj.6713/fig-2

P. falciparum (Hoepfner et al., 2012; Rottmann et al., 2010; Shaw et al., 2015; McLean & Jacobs-Lorena, 2017) led to markedly reduced puromycylation signal in both transgenic parasites, validating the assay (Fig. S5). Puromycylation signal was not significantly different in either parasite treated with GlcN for 72 h prior to puromycin labeling compared with parasites with no GlcN pre-treatment, suggesting that attenuation of *PfDHS* expression has little effect on the global translation level during this period (Fig. 3). Moreover, GlcN-treated parasites do not show any gross morphological defect (Fig. S6) and proliferation over 72 h is unaffected by GlcN (Fig. S7). These data suggest that the slight reduction of hypusination in parasites with attenuated *PfDHS* function is tolerated for short periods.

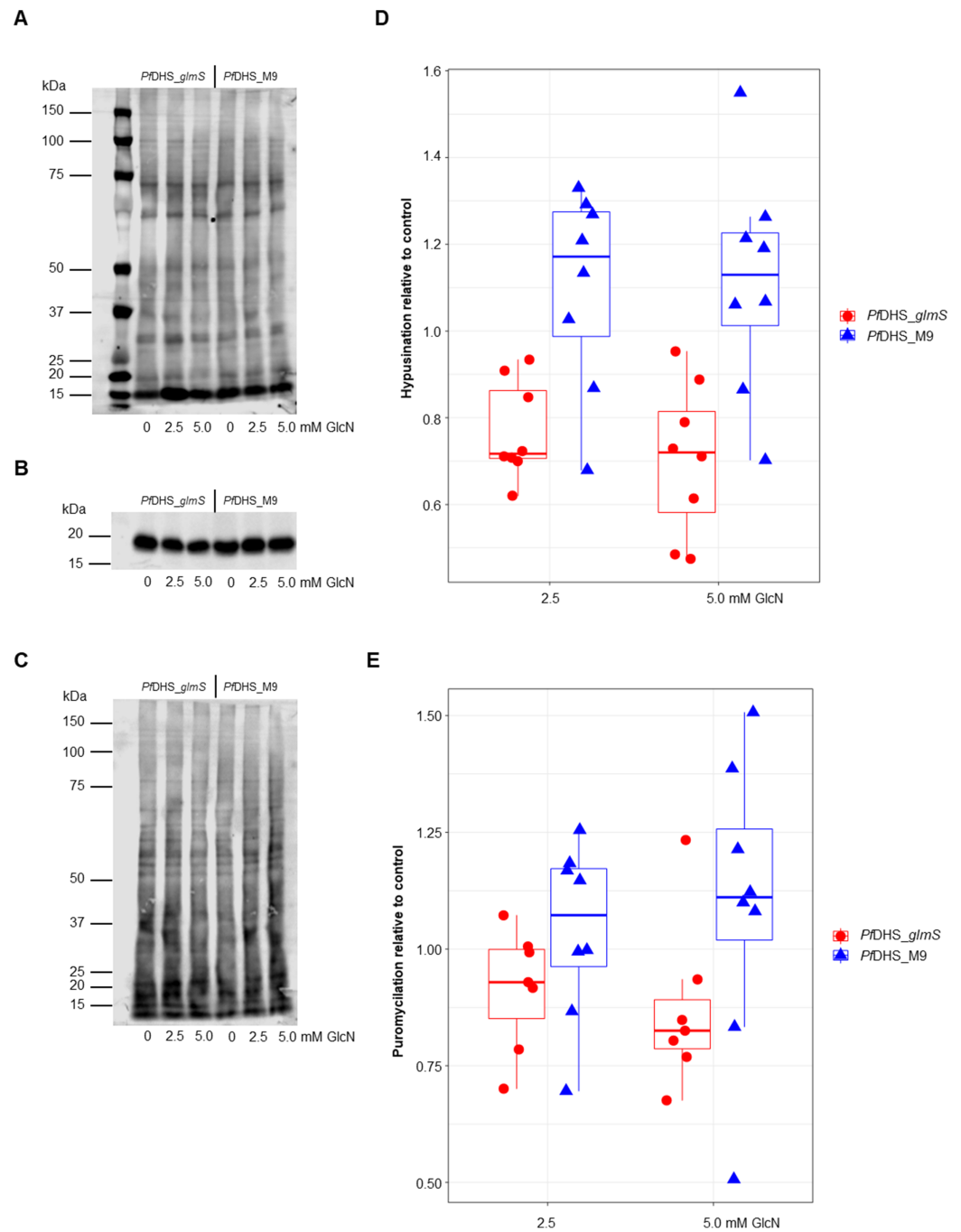



Figure 3 Hypusination and nascent protein synthesis assays. Ring-synchronized *PfDHS_glmS* and *PfDHS_M9* transgenic parasites were treated with 0, 2.5, or 5.0 mM glucosamine (GlcN) for 72 h. For assays of nascent protein synthesis, parasites were subsequently treated with 5 μ M puromycin for 10 min prior to harvesting of parasites. Protein was extracted from parasites and separated in 4–12% NuPAGE gel. Representative data are shown in parts (A–C). The images in parts (A) and (B) are cropped for clarity. Full-length, uncropped blot images are shown in Fig. S5. (A) Total protein stained with REVERT. (B) Hypusination assay results. A band corresponding to *Plasmodium falciparum* eIF5A (17.6 kDa) was detected with anti-hypusine polyclonal antibody. (C) Nascent protein synthesis assay. Puromycylated, nascent peptides were detected with anti-puromycin monoclonal antibody. (D) Quantified hypusination assay results from eight independent experiments. *P*-values from one-sample *t*-tests: 7.0e-4 (*PfDHS_glmS*, 2.5 mM GlcN); 0.0020 (*PfDHS_glmS*, 5.0 mM GlcN); 0.25 (*PfDHS_M9*, 2.5 mM GlcN),

Figure 3 (continued)

and 0.25 (*PfDHS_M9*, 5.0 mM GlcN). (E) Quantified puromycilation assay results from seven (*PfDHS_glmS*) and eight (*PfDHS_M9*) independent experiments. *P*-values from one-sample *t*-tests: 0.13 (*PfDHS_glmS*, 2.5 mM GlcN); 0.10 (*PfDHS_glmS*, 5.0 mM GlcN); 0.58 (*PfDHS_M9*, 2.5 mM GlcN), and 0.42 (*PfDHS_M9*, 5.0 mM GlcN). [Full-size](#)  DOI: 10.7717/peerj.6713/fig-3

Although attenuation of *PfDHS* gene expression is not deleterious in the short term, prolonged loss of *PfDHS* activity could lead to a growth defect. In the standard growth assay, parasite cultures are initiated at low parasite density, for example, 0.1% parasitemia, and growth assessed over the first two cycles (up to 96 h). For some essential genes, *glmS* riboswitch-mediated attenuation of expression can cause a significant growth defect under these conditions, for example, *PfDHFR-TS* (*Prommana et al., 2013*), *PfPTEX150* (*Elsworth et al., 2014*), *PfRhopH2* (*Counihan et al., 2017*; *Ito, Schureck & Desai, 2017*) and *PfRhopH3* (*Ito, Schureck & Desai, 2017*). However, *glmS* riboswitch-mediated attenuation of other essential genes such as *PfPMV* (*Sleebbs et al., 2014*) and *PfFP3* (*Xie et al., 2016*) failed to show a growth defect in the standard growth assay. The inability to detect growth defects in the standard growth assay is due to factors such as insufficient attenuation, functional overlap/redundancy with related proteins and stage-specific target protein function. For growth assays longer than two cycles, dilution of cells is necessary to prevent overgrowth of controls. Transgenic parasites obtained by single cross-over recombination must be maintained under a drug selective regimen, for example, blasticidin, otherwise they can be outgrown by wild-type revertants. To account for possible growth confounding effect of the transgenic selective regimen, a control transgenic parasite (*PfFC_glmS*) was created with integration of the *glmS* riboswitch at the ferrochelatase (*PfFC*) gene. The *PfFC* gene is dispensable during intra-erythrocytic stages, since the growth of clonal transgenic parasites with knockout of this gene is not significantly different from wild-type (*Ke et al., 2014*; *Sigala et al., 2015*). We could not assess localization or riboswitch-mediated attenuation of *PfFC*-GFP protein in the *PfFC_glmS* parasite, since no green fluorescent *PfFC_glmS* parasites were observed by microscopy (*Fig. S8*), and the weak signal of putative *PfFC*-GFP protein was difficult to distinguish from background in Western immunoblotting experiments (*Fig. S9*). We validated the *PfFC_glmS* parasite as a control in growth experiments by assessing its growth in comparison with 3D7 wild-type parasite under different GlcN treatments. Over the course of 10 growth cycles, treatment with 2.5 or 5.0 mM GlcN has no significant effect on ring or trophozoite development for both 3D7 and *PfFC_glmS* parasites (*Fig. S10*).

We established a competitive growth assay in which transgenic parasites are cultured for 10 growth cycles. The extended growth period in this assay allows for detection of latent defects that are apparent only after several growth cycles have elapsed. In this assay, a test transgenic parasite is co-cultured with the control *PfFC_glmS* transgenic parasite. The growth of test transgenic parasite was assessed by measuring the test:control transgenic parasite ratio by qPCR. The use of the control *PfFC_glmS* parasite allowed us to monitor growth without correction of dilution factors. Relative growth of the *PfDHS_glmS*

parasite was significantly reduced under GlcN treatment (Fig. 4A). In contrast, GlcN had no significant effect on the relative growth of the *PfDHS_M9* parasite (Fig 4B). Competitive growth assay of the *PfDHFR-TS_glmS* parasite revealed a more severe growth defect when treated with GlcN in which *PfDHFR-TS_glmS* parasites declined more rapidly (Fig. 4C). The results from competitive growth assays showed that attenuation of *PfDHS* expression causes a growth defect, indicating that this gene is likely to be essential. As a further test of this gene's essentiality and validation as an antimalarial target, chemogenomic profiling using antimalarial compounds was performed. In this approach, *glmS* riboswitch-mediated attenuation of target gene expression sensitizes the parasite to antimalarials acting on that target (Aroonsri et al., 2016). Chemogenomic profiling of transgenic parasites was performed with growth-inhibitory compounds differing in their mode of action (Fig. 4D). The *PfDHS_glmS* parasite is significantly more sensitive to GC7, a known inhibitor of *PfDHS* enzyme activity in vitro (Kaiser et al., 2007), when co-treated with GlcN. We noted though that the \log_2 EC₅₀ (-GlcN/+GlcN) ratio is less than one for the *PfDHS_glmS* parasite. In contrast, the *PfDHS_M9* parasite is not significantly more sensitive to GC7 when co-treated with GlcN. GlcN co-treatment does not significantly increase the sensitivity of either parasite to control drugs which do not target the *PfDHS*, including CYC, a known inhibitor of the ribosome (Obrig et al., 1971; Schneider-Poetsch et al., 2010), and PYR, which targets *PfDHFR-TS* (Aroonsri et al., 2016).

In order to assess the feasibility of *PfDHS* as a target for rationally designed inhibitors, structural study was performed. A three-dimensional structure of *PfDHS* was constructed by homology modeling using a human DHS crystal structure (Fig. 5). The quality of the *PfDHS* structure core is estimated to be high with most residues showing QMEAN scores greater than 0.7. The periphery of the *PfDHS* structure is of lower estimated quality owing to inserts not present in the human DHS protein (Fig. S12). Ligand binding site analysis identified two binding sites with significantly high scores. The top-scoring site with a site score of 1.16 corresponds to the putative substrate binding pocket occupied by spermidine or a competitive inhibitor such as GC7. The tetramer substrate binding pockets are arranged in a sandwich homodimer manner with two sites per homodimer interface (Fig. 6A). The substrate binding pockets in each *PfDHS* subunit are connected in a tunnel-like fashion highly similar to human DHS (Fig. 6B). Comparison of residues in the vicinity of the substrate binding pocket between *PfDHS* and human DHS revealed conservation of key interacting residues in *PfDHS* including Asp368, Asn420, Gly442, Ser443, and Glu451 (Fig. 6C). SiteMap also identified other residues conserved between human and *PfDHS* that may interact with GC7, or contribute to the environment favorable for GC7 binding (Figs. 6D and 6E). SiteMap detected a second ligand binding site in *PfDHS* with a site score of 1.01. This site is located in-between the two insertion loops of *PfDHS* and adjacent to a putative ball-and-chain motif (Fig. S13). The ball-and-chain motif regulates access to the substrate binding pocket, and becomes disordered upon substrate or inhibitor binding (Liao et al., 1998; Umland et al., 2004).

Hypusinated eIF5A is thought to be important for translation elongation at poorly translated codons, especially consecutive proline-coding codons (Dever, Gutierrez & Shin, 2014).

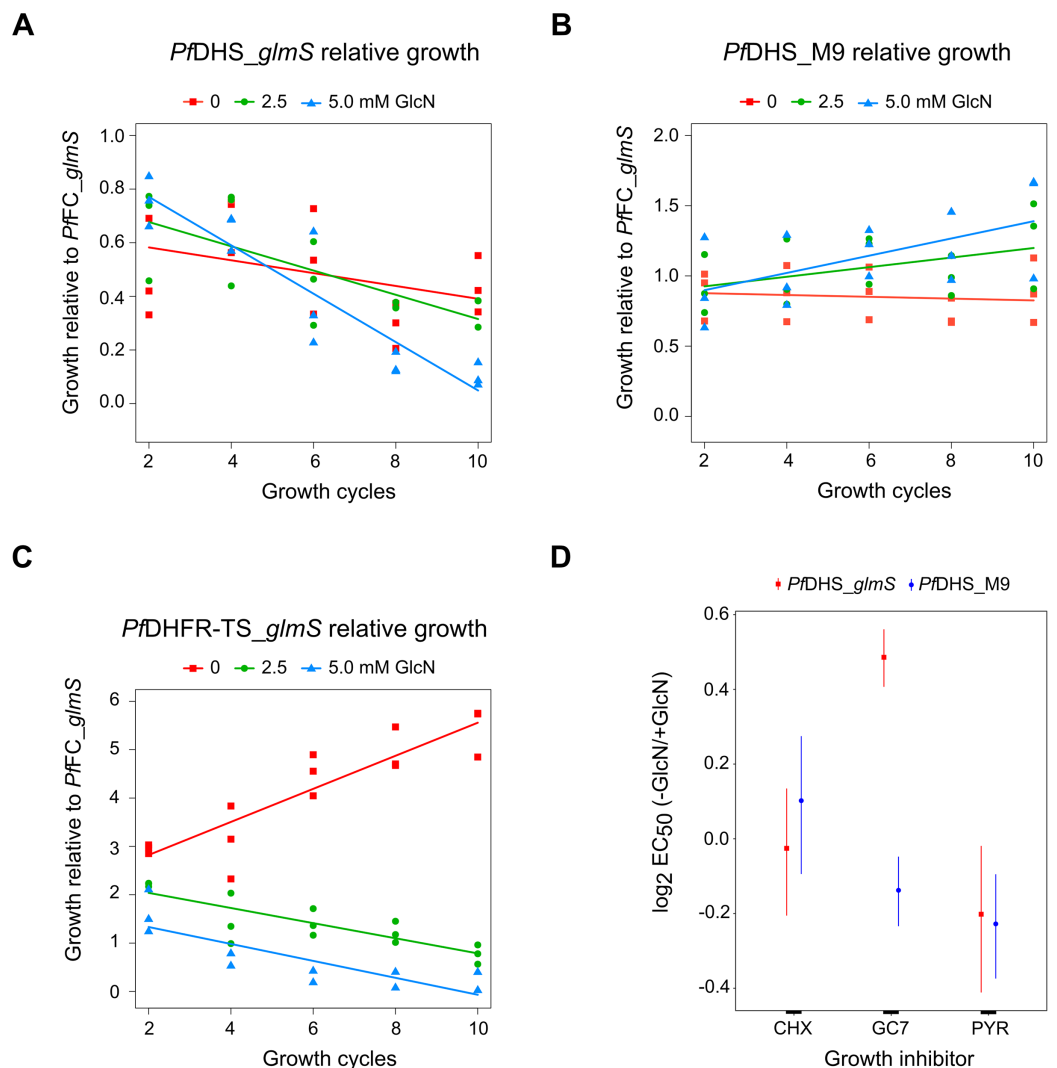


Figure 4 Growth phenotypes of transgenic parasites. Effects of glucosamine (GlcN) on the growth of transgenic parasites in co-culture experiments are shown in parts (A–C). Test transgenic parasites *PfDHS_glmS* (A), *PfDHS_M9* (B) and *PfDHFR-TS_glmS* (C) were combined with control *PfFC_glmS* parasites in a 1:1 ratio and co-cultured. Samples were taken from the culture every two growth cycles until the tenth cycle. The ratio of test:control transgenic parasite at each time-point was determined by qPCR using primers specific for each transgenic parasite. This ratio was taken as the relative growth value for modelling. The data from three independent experiments for each condition are shown. The lines on the graphs are the linear mixed effect models of growth at the indicated treatment doses of GlcN. *P*-values from likelihood ratio test: 0.0024 (*PfDHS_glmS*); 0.19 (*PfDHS_M9*); 3.9e-11 (*PfDHFR-TS_glmS*). Part (D) shows the effect of GlcN on modulating transgenic parasite sensitivity to growth inhibitory compounds. Dose-response assays were performed with (2.5 mM) or without GlcN co-treatment. Three or four independent experiments were performed for each condition. The growth inhibitory compounds tested included cycloheximide (CHX), *N*¹-guanyl-1,7-diaminoheptane (GC7) and pyrimethamine (PYR). The 50% inhibitory concentration of each compound (EC_{50}) was determined by analysis of dose-response data for *PfDHS_glmS* and *PfDHS_M9* transgenic parasites. The dose-response data and fitted curves are shown in Fig. S11. The estimated \log_2 ratio of EC_{50} between the –GlcN and +GlcN conditions together with CI_{95} is shown for each compound and transgenic parasite. *P*-values comparing $\log_2 EC_{50} (-GlcN/+GlcN)$ estimates: 0.76 (*PfDHS_glmS*, CHX); 2.0e-15 (*PfDHS_glmS*, GC7); 0.030 (*PfDHS_glmS*, PYR); 0.28 (*PfDHS_M9*, CHX); 0.0031 (*PfDHS_M9*, GC7); 9.0e-4 (*PfDHS_M9*, PYR).

Full-size DOI: 10.7717/peerj.6713/fig-4

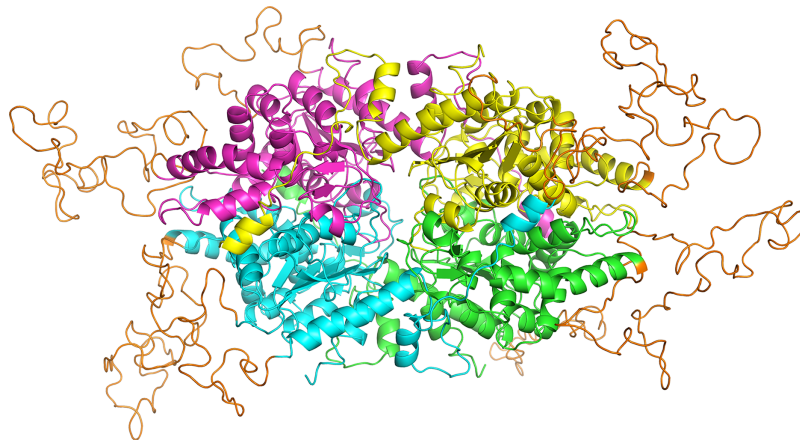


Figure 5 Homology model of *PfDHS* structure. The modeled *PfDHS* structure is a tetramer of subunits. The subunit cores are colored in magenta, yellow, cyan, and green. *PfDHS* insertion loops with no homologous residues in human DHS are colored in orange. The alignment of *PfDHS* with human DHS template (PDB: 1RLZ) is shown in Fig. S12. [Full-size](#) DOI: 10.7717/peerj.6713/fig-5

Polyproline motifs are numerous in unicellular eukaryotes such as *Saccharomyces cerevisiae* yeast with 769 genes containing PPP or PPG coding motifs (Mandal, Mandal & Park, 2014). Moreover, 136/1110 of yeast essential genes (Zhang, 2004) contain polyproline coding motifs. The essential genes with polyproline motifs therefore represent 136/5175 (2.6%) of the total yeast protein-coding genes. We therefore performed a bioinformatic survey of the *P. falciparum* proteome for proteins with polyproline motifs that may require hypusinated eIF5A for optimal synthesis following a previous rationale (Mandal, Mandal & Park, 2014). 257 proteins with PPP or PPG motifs were found (Table S2), of which insertions of *piggyBac* transposon are not tolerated in the corresponding coding regions for 128 genes (Zhang et al., 2018). Using the rationale that *P. falciparum* genes devoid of *piggyBac* transposon insertions are essential, 128/2680 essential genes thus contain polyproline-coding motifs. The essential genes with polyproline motifs in *P. falciparum* therefore represent a similar proportion of the total protein coding genes (128/5305; 2.4%) as in yeast. Among the 142 orthologous genes also with polyproline coding motifs in *P. berghei*, 58 are essential, 16 cause slow growth when disrupted, and 18 are dispensable (Bushell et al., 2017).

DISCUSSION

Hypusine modification of eIF5A is essential in different eukaryotic organisms. In this study, we have validated the DHS enzyme, which is responsible for the first step in the hypusination pathway, as an antimalarial target in *P. falciparum*. We created transgenic parasites with modification of the *PfDHS* gene for phenotypic study. The modification included a C-terminal GFP tag, which facilitated monitoring of *PfDHS* protein. Confocal microscopy revealed a cytoplasmic localization of GFP-tagged *PfDHS* protein, which is consistent with the localization of the mammalian DHS protein (Sievert et al., 2012). The cytoplasmic localization may be important to localize eIF5A protein, as DHS-knockout mice show accumulation of nuclear eIF5A (Pällmann et al., 2015).

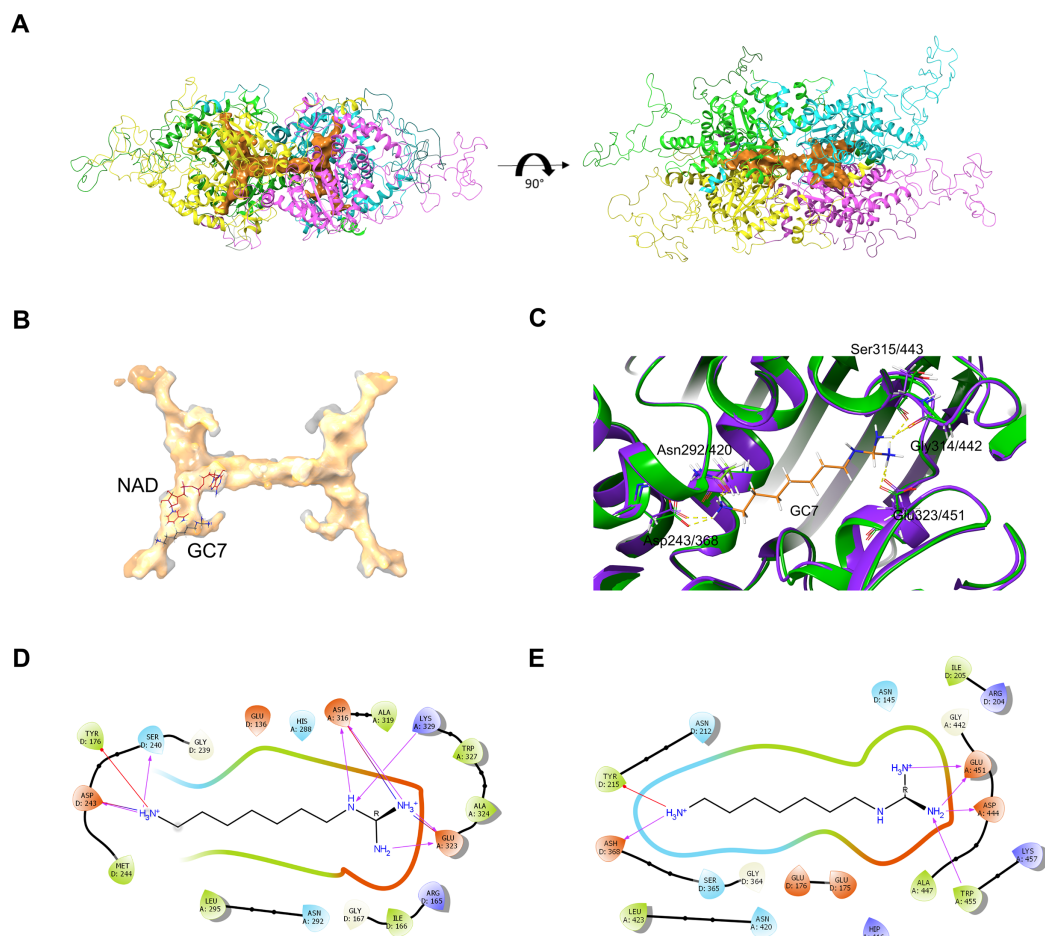


Figure 6 *PfDHS* putative substrate binding pocket and GC7 interaction. (A) *PfDHS* homology model with the top scoring ligand binding site identified by SiteMap in orange. *PfDHS* tetramer subunits are colored in magenta, yellow, cyan, and green. An alternative view of the same structure rotated 90 degrees is shown on the right. (B) Superposition of the human DHS (PDB: 1RQD) substrate binding pocket (gray) with *PfDHS* top scoring ligand binding site identified by SiteMap (orange). The NAD and GC7 molecules co-complexed with human DHS are shown for one subunit. (C) Superposition of the human DHS (PDB: 1RQD) GC7 binding domain (green) and corresponding region in *PfDHS* (purple). Key conserved DHS residues interacting with GC7 are shown, with numbering of human DHS residues followed by the *PfDHS* counterpart. (D) Interaction map of human DHS and (E) *PfDHS* residues in the GC7 binding domain. Residues are numbered according to which subunit (A–D) they belong to. Interactions between residues and GC7 are shown by arrows. Red arrow depicts π cation, blue arrows salt-bridge and magenta arrows hydrogen bond interactions.

Full-size DOI: 10.7717/peerj.6713/fig-6

We were able to attenuate *PfDHS* expression approximately fivefold in the *PfDHS_glmS* parasite with similar efficiency to that obtained for other essential genes using the same reverse-genetic system (Prommana et al., 2013; Sleebs et al., 2014; Elsworth et al., 2014; Xie et al., 2016; Counihan et al., 2017; Thériault & Richard, 2017). The attenuation of *PfDHS* expression in this transgenic parasite is specifically induced by GlcN treatment, since GlcN does not reduce expression of the same gene in the *PfDHS_M9* parasite, which differs only by two nucleotide substitutions at the *glmS* riboswitch cleavage site that nullify RNA self-cleavage (Winkler et al., 2004).

Attenuation of *PfDHS* expression in the *PfDHS_glmS* causes a growth defect, although the decline of *PfDHS_glmS* parasites in culture is less rapid than *PfDHFR-TS*-attenuated parasites. These data suggest that *PfDHS* is essential and explain why no insertions of *piggyBac* transposon are tolerated in this gene (Zhang *et al.*, 2018). However, inducible null mutants (e.g., created by using the DiCre inducible knockout method (Collins *et al.*, 2013)) are required for definitive proof of essentiality. The slow decline of *PfDHS*-attenuated parasites suggests that the residual hypusinated protein is sufficient to support viability for at least one growth cycle, perhaps because hypusinated protein is long-lived. In support of this explanation, the level of hypusinated protein in *PfDHS*-attenuated parasites is modestly reduced. A total of 60% reduction of hypusinated eIF5A in a conditional mutant of yeast with attenuated DHS expression is deleterious (Galvão *et al.*, 2013), suggesting that a certain level of hypusinated eIF5A is necessary for eukaryote cell growth. Alternatively, the growth defect in *PfDHS*-attenuated parasites could be due to loss of hypusination and/or a “moonlighting” function of *PfDHS*. To test possible “moonlighting” functions of *PfDHS*, data from catalytically inactive *PfDHS* mutants are required. Although the slow decline of *PfDHS*-attenuated parasites could be attributed to incomplete attenuation of *PfDHS* expression, decline of null *PfDHS* mutants in growth assays may not be much more rapid since null DHS mutants of yeast can undergo several cell divisions before arrest (Park, Joe & Kang, 1998).

The competitive growth assay developed in this study is suitable for monitoring of growth over extended periods and demonstrating latent (more than two growth cycles) growth defects. Our method has the advantage that no correction for dilution factors is necessary, which could introduce substantial error. However, we have not performed head to head comparisons of the competitive growth assay with other methods to assess accuracy. The competitive growth assay could be scaled-up by pooling parasites with *glmS* riboswitch modifications of different genes and monitoring the growth of each mutant by next-generation sequencing, similar to that described for mutants carrying *piggyBac* insertions (Bronner *et al.*, 2016). The competitive growth assay is an alternative to the plaque-based growth assay, which has been used to demonstrate latent growth defects in essential invasion genes (Thomas *et al.*, 2016). The small size of plaques make quantification difficult, especially if a scanner of sufficiently high resolution is not available. Slow growing mutant parasites may also have failed to reach a sufficiently critical mass at the end of the assay period such that no plaque is visible and the growth defect over-estimated. The growth defects of mutant parasites inferred from plaque assay can be confounded by competition with wild-type parasites (Lehmann *et al.*, 2018). Furthermore, the plaque-based growth assay is an end-point assay and so cannot provide information of growth dynamics like the competitive growth assay.

From the latent growth defect in *PfDHS* mutants, *PfDHS* can be considered a less vulnerable antimalarial target than other essential genes such as *PfDHFR-TS*. Information of target vulnerability is important for antimalarial development. It may be difficult to develop potent antimalarial derivatives from hit compounds obtained by high throughput screening if the target has a low vulnerability. This is because inhibitors of less vulnerable targets need to bind the target with very high affinity to ensure that almost

all target activity is inhibited at therapeutic doses for antimalarial efficacy. In contrast, compounds against the most vulnerable targets (for which even small reductions in activity are deleterious to the parasite) may only need to have moderate binding affinity for high antimalarial efficacy. Furthermore, knowledge of target vulnerability could be important for consideration of how easily resistance could evolve. Resistance mutations in less vulnerable targets that cause a small reduction of inhibitor binding affinity could render drugs ineffective. If a panel of mutants with the expression of different essential genes attenuated using the *glmS* riboswitch or another reverse genetic tool was available, competitive growth assays could be performed to systematically compare target vulnerabilities and triage targets for antimalarial development.

PfDHS-attenuated parasites are significantly more sensitive to growth inhibition by GC7, suggesting that the primary *in vivo* target of this compound is *PfDHS*. The slow decline of genetically attenuated *PfDHS* parasites in competitive growth assays suggests that some of the antimalarial effect of GC7 observed in standard antimalarial assays, in which growth is assessed over shorter periods, could be attributed to inhibition of secondary targets (off-targeting). The \log_2 EC₅₀ (-GlcN/+GlcN) ratio for GC7 against the *PfDHS_glmS* parasite is markedly lower than the ratios for antifolates against the *PfDHFR-TS_glmS* parasite (Aroonsri *et al.*, 2016). Low EC₅₀ ratios are consistent with off-targeting. In support of this inference, GC7 has reported off-target effects in human cells, including induction of autophagy independently of eIF5A activity (Oliverio *et al.*, 2014). Alternatively, the low EC₅₀ ratio for GC7 against the *PfDHS_glmS* parasite may not be due to off-targeting if the level of *PfDHS* activity remaining in the +GlcN condition is still in excess of what is required for growth.

The inference that *PfDHS* is the primary antimalarial target of GC7 is supported by the *in silico* modeling data, which show conservation of substrate binding pocket and *PfDHS* residues putatively involved with GC7 interaction. The high conservation of substrate binding pocket could make the design of antimalarials specific to the *PfDHS* target challenging. However, the modeled *PfDHS* structure reveals a second potential ligand binding site that could also be exploited for rational drug design. The second site overlaps insert residues not present in human DHS and a putative ball-and-chain motif. Compounds binding to this site thus could act as allosteric inhibitors by preventing access of protein substrates to the substrate binding pocket for deoxyhypusine modification. X-ray structural data of *PfDHS* could provide important insights into *PfDHS* for drug design not revealed by *in silico* modeling, including the roles of the ball-and-chain motif and inserts peripheral to the core.

The primary function of hypusinated eIF5A for translation elongation, particularly of polyproline motifs may be conserved in *P. falciparum*, as a number of its proteins contain these motifs. Although *P. falciparum* has markedly fewer polyproline-motif proteins than yeast, the number of these proteins that are essential with respect to the total protein complement is similar. Insufficient synthesis of one or more essential protein could be responsible for the growth defect in *PfDHS* attenuated mutants, although proteomic data are needed to test this hypothesis. The small number of polyproline motif proteins

in *P. falciparum* that potentially require hypusinated *Pf*eIF5A for their production could explain why global protein synthesis (in the short term) is not significantly reduced when *Pf*DHS function is attenuated.

CONCLUSIONS

The loss of *Pf*DHS function leads to a growth defect, suggesting that this gene is essential. However, definitive proof from null mutants is required to conclude essentiality. Loss of *Pf*DHS function leads to reduction of hypusination, which may affect synthesis of some proteins. *Pf*DHS is not as vulnerable a target as other essential genes such as *Pf*DHFR-TS, although it can be targeted by antimalarials such as GC7.

ADDITIONAL INFORMATION AND DECLARATIONS

Funding

We received funding from the Thailand Research Fund grant nos. RSA5780007, RSA5880064, and TRG6080001 to Philip. J. Shaw, Chairat Uthaipibull and Aiyada Aroonsri respectively; National Science and Technology Development Agency (NSTDA) (Thailand) project nos. P1450752, P1300832, P1450883, P1751076 to Philip. J. Shaw, Chairat Uthaipibull, Sumalee Kamchonwongpaisan and Aiyada Aroonsri, respectively; NSTDA Core Researcher Grant no. P1850116 to Sumalee Kamchonwongpaisan and BIOTEC (Thailand) Young Fellow Research Grant no. P1750543 to Aiyada Aroonsri. The funders had no role in study design, data collection and analysis, decision to publish, or preparation of the manuscript.

Grant Disclosures

The following grant information was disclosed by the authors:

Thailand Research Fund: RSA5780007, RSA5880064, and TRG6080001.

National Science and Technology Development Agency (NSTDA) (Thailand) project: P1450752, P1300832, P1450883, P1751076.

NSTDA Core Researcher: P1850116.

BIOTEC Young Fellow Research Grant: P1750543.

Competing Interests

The authors declare that they have no competing interests.

Author Contributions

- Aiyada Aroonsri conceived and designed the experiments, performed the experiments, analyzed the data, prepared figures and/or tables, authored or reviewed drafts of the paper, approved the final draft.
- Navaporn Posayapisit conceived and designed the experiments, performed the experiments, analyzed the data, prepared figures and/or tables, authored or reviewed drafts of the paper, approved the final draft.
- Jindaporn Kongsee performed the experiments, approved the final draft.
- Onsiri Siripan performed the experiments, approved the final draft.

- Danoo Vitsupakorn conceived and designed the experiments, performed the experiments, prepared figures and/or tables, approved the final draft.
- Sugunya Utaida performed the experiments, authored or reviewed drafts of the paper, approved the final draft.
- Chairat Uthaipibull analyzed the data, authored or reviewed drafts of the paper, approved the final draft.
- Sumalee Kamchonwongpaisan analyzed the data, authored or reviewed drafts of the paper, approved the final draft.
- Philip J. Shaw conceived and designed the experiments, performed the experiments, analyzed the data, prepared figures and/or tables, authored or reviewed drafts of the paper, approved the final draft.

Human Ethics

The following information was supplied relating to ethical approvals (i.e., approving body and any reference numbers):

Human erythrocytes were obtained from donors after providing informed written consent, following a protocol approved by the Ethics Committee, National Science and Technology Development Agency, Pathum Thani, Thailand, document no. 0021/2560.

Data Availability

The following information was supplied regarding data availability:

The raw data are included in the figures and [Supplemental Files](#).

Supplemental Information

Supplemental information for this article can be found online at <http://dx.doi.org/10.7717/peerj.6713#supplemental-information>.

REFERENCES

- Aroonsri A, Akinola O, Posayapisit N, Songsunghong W, Uthaipibull C, Kamchonwongpaisan S, Gbotosho GO, Yuthavong Y, Shaw PJ. 2016. Identifying antimalarial compounds targeting dihydrofolate reductase-thymidylate synthase (DHFR-TS) by chemogenomic profiling. *International Journal for Parasitology* **46**(8):527–535 DOI [10.1016/j.ijpara.2016.04.002](https://doi.org/10.1016/j.ijpara.2016.04.002).
- Bates D, Mächler M, Bolker B, Walker S. 2015. Fitting linear mixed-effects models using lme4. *Journal of Statistical Software* **67**(1):1–48 DOI [10.18637/jss.v067.i01](https://doi.org/10.18637/jss.v067.i01).
- Breheny P, Burchett W. 2017. Visualization of regression models using visreg. *R Journal* **9**(2):56–71.
- Bronner IFF, Ottoa TD, Zhang M, Udenze K, Wang CCQ, Quail MA, Jiang RHY, Adams JH, Rayner JC. 2016. Quantitative insertion-site sequencing (QIseq) for high throughput phenotyping of transposon mutants. *Genome Research* **26**(7):980–989 DOI [10.1101/gr.200279.115](https://doi.org/10.1101/gr.200279.115).
- Bushell E, Gomes AR, Sanderson T, Anar B, Girling G, Herd C, Metcalf T, Modrzynska K, Schwach F, Martin RE, Mather MW, McFadden GI, Parts L, Rutledge GG, Vaidya AB, Wengelnik K, Rayner JC, Billker O. 2017. Functional profiling of a plasmodium

genome reveals an abundance of essential genes. *Cell* **170**(2):260–272.e8

DOI [10.1016/j.cell.2017.06.030](https://doi.org/10.1016/j.cell.2017.06.030).

- Clark K, Niemand J, Reeksting S, Smit S, Van Brummelen AC, Williams M, Louw AI, Birkholtz L. 2010.** Functional consequences of perturbing polyamine metabolism in the malaria parasite, *Plasmodium falciparum*. *Amino Acids* **38**(2):633–644
DOI [10.1007/s00726-009-0424-7](https://doi.org/10.1007/s00726-009-0424-7).
- Collins CR, Das S, Wong EH, Andenmatten N, Stallmach R, Hackett F, Herman J-P, Müller S, Meissner M, Blackman MJ. 2013.** Robust inducible Cre recombinase activity in the human malaria parasite *Plasmodium falciparum* enables efficient gene deletion within a single asexual erythrocytic growth cycle. *Molecular Microbiology* **88**(4):687–701
DOI [10.1111/mmi.12206](https://doi.org/10.1111/mmi.12206).
- Counihan N, Chisholm SA, Bullen HE, Srivastava A, Sanders PR, Jonsdottir TK, Weiss GE, Ghosh S, Crabb BS, Creek DJ, Gilson PR, de Koning-Ward TF. 2017.** *Plasmodium falciparum* parasites deploy RhopH2 into the host erythrocyte to obtain nutrients, grow and replicate. *eLife* **6**:e23217 DOI [10.7554/eLife.23217](https://doi.org/10.7554/eLife.23217).
- Cranmer SL, Magowan C, Liang J, Coppel RL, Cooke BM. 1997.** An alternative to serum for cultivation of *Plasmodium falciparum* in vitro. *Transactions of the Royal Society of Tropical Medicine and Hygiene* **91**(3):363–365 DOI [10.1016/S0035-9203\(97\)90110-3](https://doi.org/10.1016/S0035-9203(97)90110-3).
- Deitsch K, Driskill C, Wellems T. 2001.** Transformation of malaria parasites by the spontaneous uptake and expression of DNA from human erythrocytes. *Nucleic Acids Research* **29**(3):850–853
DOI [10.1093/nar/29.3.850](https://doi.org/10.1093/nar/29.3.850).
- Dever TE, Gutierrez E, Shin B-S. 2014.** The hypusine-containing translation factor eIF5A. *Critical Reviews in Biochemistry and Molecular Biology* **49**(5):413–425
DOI [10.3109/10409238.2014.939608](https://doi.org/10.3109/10409238.2014.939608).
- Elsworth B, Matthews K, Nie CQ, Kalanon M, Charnaud SC, Sanders PR, Chisholm SA, Counihan NA, Shaw PJ, Pino P, Chan J-A, Azevedo MF, Rogerson SJ, Beeson JG, Crabb BS, Gilson PR, de Koning-Ward TF. 2014.** PTEX is an essential nexus for protein export in malaria parasites. *Nature* **511**(7511):587–591 DOI [10.1038/nature13555](https://doi.org/10.1038/nature13555).
- Foth BJ, Zhang N, Mok S, Preiser PR, Bozdech Z. 2008.** Quantitative protein expression profiling reveals extensive post-transcriptional regulation and post-translational modifications in schizont-stage malaria parasites. *Genome Biology* **9**:R177 DOI [10.1186/gb-2008-9-12-r177](https://doi.org/10.1186/gb-2008-9-12-r177).
- Friesner RA, Banks JL, Murphy RB, Halgren TA, Klicic JJ, Mainz DT, Repasky MP, Knoll EH, Shelley M, Perry JK, Shaw DE, Francis P, Shenkin PS. 2004.** Glide: a new approach for rapid, accurate docking and scoring. 1. Method and assessment of docking accuracy. *Journal of Medicinal Chemistry* **47**(7):1739–1749 DOI [10.1021/jm0306430](https://doi.org/10.1021/jm0306430).
- Galvão FC, Rossi D, Da Silveira WS, Valentini SR, Zanelli CF. 2013.** The deoxyhypusine synthase mutant dys1-1 reveals the association of eIF5A and Asc1 with cell wall integrity. *PLOS ONE* **8**(4):e60140 DOI [10.1371/journal.pone.0060140](https://doi.org/10.1371/journal.pone.0060140).
- Halgren TA. 2009.** Identifying and characterizing binding sites and assessing druggability. *Journal of Chemical Information and Modeling* **49**(2):377–389
DOI [10.1021/ci800324m](https://doi.org/10.1021/ci800324m).
- Hoepfner D, McNamara CW, Lim CS, Studer C, Riedl R, Aust T, McCormack SL, Plouffe DM, Meister S, Schuierer S, Plikat U, Hartmann N, Staedtler F, Cotesta S, Schmitt EK, Petersen F, Supek F, Glynn RJ, Tallarico JA, Porter JA, Fishman MC, Bodenreider C, Diagana TT, Movva NR, Winzeler EA. 2012.** Selective and specific inhibition of the *Plasmodium falciparum* Lysyl-tRNA synthetase by the fungal secondary metabolite cladosporin. *Cell Host & Microbe* **11**(6):654–663 DOI [10.1016/j.chom.2012.04.015](https://doi.org/10.1016/j.chom.2012.04.015).

- Ito D, Schureck MA, Desai SA. 2017. An essential dual-function complex mediates erythrocyte invasion and channel-mediated nutrient uptake in malaria parasites. *eLife* 6:e23485 DOI 10.7554/eLife.23485.
- Kaiser A, Gottwald A, Wiersch C, Lindenthal B, Maier W, Seitz HM. 2001. Effect of drugs inhibiting spermidine biosynthesis and metabolism on the in vitro development of *Plasmodium falciparum*. *Parasitology Research* 87(11):963–972 DOI 10.1007/s004360100460.
- Kaiser A, Hammels I, Gottwald A, Nassar M, Zaghoul MS, Motaal BA, Hauber J, Hoerauf A. 2007. Modification of eukaryotic initiation factor 5A from *Plasmodium vivax* by a truncated deoxyhypusine synthase from *Plasmodium falciparum*: An enzyme with dual enzymatic properties. *Bioorganic & Medicinal Chemistry* 15(18):6200–6207 DOI 10.1016/j.bmc.2007.06.026.
- Ke H, Sigala PA, Miura K, Morrissey JM, Mather MW, Crowley JR, Henderson JP, Goldberg DE, Long CA, Vaidya AB. 2014. The heme biosynthesis pathway is essential for *Plasmodium falciparum* development in mosquito stage but not in blood stages. *Journal of Biological Chemistry* 289(50):34827–34837 DOI 10.1074/jbc.M114.615831.
- Kersting D, Krüger M, Sattler JM, Mueller A-K, Kaiser A. 2016. A suggested vital function for eIF-5A and dhs genes during murine malaria blood-stage infection. *FEBS Open Bio* 6(8):860–872 DOI 10.1002/2211-5463.12093.
- Lambros C, Vanderberg JP. 1979. Synchronization of *Plasmodium falciparum* erythrocytic stages in culture. *Journal of Parasitology* 65(3):418–420 DOI 10.2307/3280287.
- Lehmann C, Tan MSY, De Vries LE, Russo I, Sanchez MI, Goldberg DE, Deu E. 2018. *Plasmodium falciparum* dipeptidyl aminopeptidase 3 activity is important for efficient erythrocyte invasion by the malaria parasite. *PLOS Pathogens* 14(5):e1007031 DOI 10.1371/journal.ppat.1007031.
- Liao DI, Wolff EC, Park MH, Davies DR. 1998. Crystal structure of the NAD complex of human deoxyhypusine synthase: an enzyme with a ball-and-chain mechanism for blocking the active site. *Structure* 6(1):23–35 DOI 10.1016/S0969-2126(98)00004-5.
- Mandal A, Mandal S, Park MH. 2014. Genome-wide analyses and functional classification of proline repeat-rich proteins: potential role of eIF5A in Eukaryotic evolution. *PLOS ONE* 9(11):e111800 DOI 10.1371/journal.pone.0111800.
- McLean KJ, Jacobs-Lorena M. 2017. *Plasmodium falciparum* *Maf1* confers survival upon amino acid starvation. *mBio* 8(2):e02317-16 DOI 10.1128/mBio.02317-16.
- Molitor IM, Knöbel S, Dang C, Spielmann T, Alléra A, König GM. 2004. Translation initiation factor eIF-5A from *Plasmodium falciparum*. *Molecular and Biochemical Parasitology* 137(1):65–74 DOI 10.1016/j.molbiopara.2004.04.013.
- Nathans D. 1964. Puromycin inhibition of protein synthesis: incorporation of puromycin into peptide chains. *Proceedings of the National Academy of Sciences of the United States of America* 51(4):585–592 DOI 10.1073/pnas.51.4.585.
- Obrig TG, Culp WJ, McKeehan WL, Hardesty B. 1971. The mechanism by which cycloheximide and related glutarimide antibiotics inhibit peptide synthesis on reticulocyte ribosomes. *Journal of Biological Chemistry* 246(1):174–181.
- Oliverio S, Corazzari M, Sestito C, Piredda L, Ippolito G, Piacentini M. 2014. The spermidine analogue GC7 (N1-guanyl-1,7-diaminoheptane) induces autophagy through a mechanism not involving the hypusination of eIF5A. *Amino Acids* 46(12):2767–2776 DOI 10.1007/s00726-014-1821-0.
- Pällmann N, Braig M, Sievert H, Preukschas M, Hermans-Borgmeyer I, Schweizer M, Nagel CH, Neumann M, Wild P, Haralambieva E, Hagel C, Bokemeyer C, Hauber J,

- Balabanov S.** 2015. Biological relevance and therapeutic potential of the hypusine modification system. *Journal of Biological Chemistry* **290**(30):18343–18360 DOI [10.1074/jbc.M115.664490](https://doi.org/10.1074/jbc.M115.664490).
- Park MH, Joe YA, Kang KR.** 1998. Deoxyhypusine synthase activity is essential for cell viability in the yeast *Saccharomyces cerevisiae*. *Journal of Biological Chemistry* **273**(3):1677–1683 DOI [10.1074/jbc.273.3.1677](https://doi.org/10.1074/jbc.273.3.1677).
- Park MH, Nishimura K, Zanelli CF, Valentini SR.** 2010. Functional significance of eIF5A and its hypusine modification in eukaryotes. *Amino Acids* **38**(2):491–500 DOI [10.1007/s00726-009-0408-7](https://doi.org/10.1007/s00726-009-0408-7).
- Prommana P, Uthaipibull C, Wongsombat C, Kamchonwongpaisan S, Yuthavong Y, Knuepfer E, Holder AA, Shaw PJ.** 2013. Inducible knockdown of *Plasmodium* gene expression using the *glmS* Ribozyme. *PLOS ONE* **8**(8):e73783 DOI [10.1371/journal.pone.0073783](https://doi.org/10.1371/journal.pone.0073783).
- R Core Team.** 2017. *R: a language and environment for statistical computing*. Vienna: The R Foundation for Statistical Computing. Available at <https://www.r-project.org/> (accessed 1 February 2019).
- Ritz C, Streibig JC.** 2005. Bioassay analysis using R. *Journal of Statistical Software* **12**(5):1–22 DOI [10.18637/jss.v012.i05](https://doi.org/10.18637/jss.v012.i05).
- Rottmann M, McNamara C, Yeung BKS, Lee MCS, Zou B, Russell B, Seitz P, Plouffe DM, Dharia NV, Tan J, Cohen SB, Spencer KR, Gonzalez-Paez GE, Lakshminarayana SB, Goh A, Suwanarusk R, Jegla T, Schmitt EK, Beck H-P, Brun R, Nosten F, Renia L, Dartois V, Keller TH, Fidock DA, Winzeler EA, Diagana TT.** 2010. Spiroindolones, a potent compound class for the treatment of Malaria. *Science* **329**(5996):1175–1180 DOI [10.1126/science.1193225](https://doi.org/10.1126/science.1193225).
- Schmidt EK, Clavarino G, Ceppi M, Pierre P.** 2009. SUNSET, a nonradioactive method to monitor protein synthesis. *Nature Methods* **6**(4):275–277 DOI [10.1038/nmeth.1314](https://doi.org/10.1038/nmeth.1314).
- Schneider CA, Rasband WS, Eliceiri KW.** 2012. NIH Image to ImageJ: 25 years of image analysis. *Nature Methods* **9**(7):671–675 DOI [10.1038/nmeth.2089](https://doi.org/10.1038/nmeth.2089).
- Schneider-Poetsch T, Ju J, Eyler DE, Dang Y, Bhat S, Merrick WC, Green R, Shen B, Liu JO.** 2010. Inhibition of eukaryotic translation elongation by cycloheximide and lactimidomycin. *Nature Chemical Biology* **6**(3):209–217 DOI [10.1038/nchembio.304](https://doi.org/10.1038/nchembio.304).
- Shaw PJ, Chaotheing S, Kaewprommal P, Piriyaongsa J, Wongsombat C, Suwannakitti N, Koonyosying P, Uthaipibull C, Yuthavong Y, Kamchonwongpaisan S.** 2015. *Plasmodium* parasites mount an arrest response to dihydroartemisinin, as revealed by whole transcriptome shotgun sequencing (RNA-seq) and microarray study. *BMC Genomics* **16**:830 DOI [10.1186/s12864-015-2040-0](https://doi.org/10.1186/s12864-015-2040-0).
- Sievert H, Venz S, Platas-Barradas O, Dhople VM, Schaletzky M, Nagel C-H, Braig M, Preukschas M, Pällmann N, Bokemeyer C, Brümmendorf TH, Pörtner R, Walther R, Duncan KE, Hauber J, Balabanov S.** 2012. Protein-protein-interaction network organization of the hypusine modification system. *Molecular & Cellular Proteomics* **11**(11):1289–1305 DOI [10.1074/mcp.M112.019059](https://doi.org/10.1074/mcp.M112.019059).
- Sigala PA, Crowley JR, Henderson JP, Goldberg DE.** 2015. Deconvoluting heme biosynthesis to target blood-stage malaria parasites. *eLife* **4**:e09143 DOI [10.7554/eLife.09143](https://doi.org/10.7554/eLife.09143).
- Sleebbs BE, Lopaticki S, Marapana DS, O'Neill MT, Rajasekaran P, Gazdik M, Günther S, Whitehead LW, Lowes KN, Barfod L, Hviid L, Shaw PJ, Hodder AN, Smith BJ, Cowman AF, Boddey JA.** 2014. Inhibition of plasmepsin V activity demonstrates its essential role in protein export, PfEMP1 display, and survival of Malaria parasites. *PLOS Biology* **12**(7):e1001897 DOI [10.1371/journal.pbio.1001897](https://doi.org/10.1371/journal.pbio.1001897).

- Teng R, Junankar PR, Bubb WA, Rae C, Mercier P, Kirk K. 2009.** Metabolite profiling of the intraerythrocytic malaria parasite *Plasmodium falciparum* by 1H NMR spectroscopy. *NMR in Biomedicine* **22**(3):292–302 DOI [10.1002/nbm.1323](https://doi.org/10.1002/nbm.1323).
- Thériault C, Richard D. 2017.** Characterization of a putative *Plasmodium falciparum* SAC1 phosphoinositide-phosphatase homologue potentially required for survival during the asexual erythrocytic stages. *Scientific Reports* **7**(1):12710 DOI [10.1038/s41598-017-12762-0](https://doi.org/10.1038/s41598-017-12762-0).
- Thomas JA, Collins CR, Das S, Hackett F, Graindorge A, Bell D, Deu E, Blackman MJ. 2016.** Development and Application of a Simple Plaque Assay for the Human Malaria Parasite *Plasmodium falciparum*. *PLOS ONE* **11**(6):e0157873 DOI [10.1371/journal.pone.0157873](https://doi.org/10.1371/journal.pone.0157873).
- Trager W, Jensen JB. 1976.** Human malaria parasites in continuous culture. *Science* **193**(4254):673–675 DOI [10.1126/science.781840](https://doi.org/10.1126/science.781840).
- Umland TC, Wolff EC, Park MH, Davies DR. 2004.** A new crystal structure of deoxyhypusine synthase reveals the configuration of the active enzyme and of an enzyme·NAD·inhibitor ternary complex. *Journal of Biological Chemistry* **279**(27):28697–28705 DOI [10.1074/jbc.M404095200](https://doi.org/10.1074/jbc.M404095200).
- Waterhouse A, Bertoni M, Bienert S, Studer G, Tauriello G, Gumienny R, Heer FT, De Beer TAP, Rempfer C, Bordoli L, Lepore R, Schwede T. 2018.** SWISS-MODEL: homology modelling of protein structures and complexes. *Nucleic Acids Research* **46**(W1):W296–W303 DOI [10.1093/nar/gky427](https://doi.org/10.1093/nar/gky427).
- Welch BL. 1947.** The generalization of ‘Student’s’ problem when several different population variances are involved. *Biometrika* **34**(1–2):28–35 DOI [10.1093/biomet/34.1-2.28](https://doi.org/10.1093/biomet/34.1-2.28).
- Winkler WC, Nahvi A, Roth A, Collins JA, Breaker RR. 2004.** Control of gene expression by a natural metabolite-responsive ribozyme. *Nature* **428**(6980):281–286 DOI [10.1038/nature02362](https://doi.org/10.1038/nature02362).
- Woodrow CJ, White NJ. 2017.** The clinical impact of artemisinin resistance in Southeast Asia and the potential for future spread. *FEMS Microbiology Reviews* **41**(1):34–48 DOI [10.1093/femsre/fuw037](https://doi.org/10.1093/femsre/fuw037).
- World Health Organization. 2016.** *World malaria report 2016*. Geneva: World Health Organization.
- Wu Y, Sifri CD, Lei HH, Su XZ, Wellems TE. 1995.** Transfection of *Plasmodium falciparum* within human red blood cells. *Proceedings of the National Academy of Sciences of the United States of America* **92**(4):973–977 DOI [10.1073/pnas.92.4.973](https://doi.org/10.1073/pnas.92.4.973).
- Xie SC, Dogovski C, Hanssen E, Chiu F, Yang T, Crespo MP, Stafford C, Batinovic S, Teguh S, Charman S, Klonis N, Tilley L. 2016.** Haemoglobin degradation underpins the sensitivity of early ring stage *Plasmodium falciparum* to artemisinins. *Journal of Cell Science* **129**(2):406–416 DOI [10.1242/jcs.178830](https://doi.org/10.1242/jcs.178830).
- Yuan L, Hao M, Wu L, Zhao Z, Rosenthal BM, Li X, He Y, Sun L, Feng G, Xiang Z, Cui L, Yang Z. 2014.** Refrigeration provides a simple means to synchronize *in vitro* cultures of *Plasmodium falciparum*. *Experimental Parasitology* **140**:18–23 DOI [10.1016/j.exppara.2014.03.010](https://doi.org/10.1016/j.exppara.2014.03.010).
- Zhang R, Ou HY, Zhang CT. 2004.** DEG: a database of essential genes. *Nucleic Acids Research* **32**(suppl_1):D271–D272 DOI [10.1093/nar/gkh024](https://doi.org/10.1093/nar/gkh024).
- Zhang M, Wang C, Otto TD, Oberstaller J, Liao X, Adapa SR, Udenze K, Bronner IF, Casandra D, Mayho M, Brown J, Li S, Swanson J, Rayner JC, Jiang RHY, Adams JH. 2018.** Uncovering the essential genes of the human malaria parasite *Plasmodium falciparum* by saturation mutagenesis. *Science* **360**(6388):eaap7847 DOI [10.1126/science.aap7847](https://doi.org/10.1126/science.aap7847).